Shell model configurational trends in odd-odd nuclei beyond ^{208}Pb

Petr Alexa
Department of Physics and Measurements, Institute of Chemical Technology, Technická 5, CZ-166 28 Prague 6, Czech Republic

Raymond K. Sheline
Chemistry and Physics Departments, Florida State University, Tallahassee, Florida 32306-3006

(Received 23 July 1997)

Experimental information on the energy distribution of states in the lowest lying configurations of selected odd-odd nuclei just beyond ^{208}Pb is summarized. In ^{210}Bi the $\pi 0h_{9/2}\otimes\nu 1g_{9/2}$ configuration and other low lying configurations all have the inverted parabola shape in a plot of energy versus spin. When additional pairs of protons and/or neutrons are added, leading to heavier odd-odd nuclei, the inverted parabola becomes more compressed. Before these trends can be completed, however, quadrupole-octupole deformation sets in. Using the generalized intermediate coupling model, it is possible to reproduce these experimental trends and then to carry them to completion in the reversed parabola (of energy versus spin) resulting from the configuration $\pi 0h_{9/2}\otimes\nu(1g_{9/2})^{-1}$ or $\pi(0h_{9/2})^{-1}\otimes\nu 1g_{9/2}$. [S0556-2813(97)02312-1]

PACS number(s): 21.10.Pc, 21.60.Cs, 27.80.+w

I. INTRODUCTION AND EXPERIMENT

The odd-odd spherical nuclei just beyond the double closed shell of ^{208}Pb are ideal for testing the n-p interaction and the corresponding energy distributions of the states of specific configurations. For this reason ^{210}Bi has been extensively studied, both experimentally [1–12] and theoretically [13–21].

The energies of all states of the lowest three configurations ($\pi 0h_{9/2}\otimes\nu 1g_{9/2}$, $\pi 0h_{9/2}\otimes\nu 0i_{11/2}$, $\pi 1f_{7/2}\otimes\nu 1g_{9/2}$) are reliably known. Each of these configurations has the inverted parabolic structure when the spins of the configuration are plotted against their energies. That is, the lowest and highest spins in the configurations are relatively low in energy, whereas the intermediate spins lie higher in energy. The nuclei just beyond ^{210}Bi are much more difficult to study because of the lack of stable or even long lived targets in the region between ^{210}Bi and ^{226}Ra. For this reason much less experimental work is available, and the data are much more sparse.

Recently, we have studied the nuclei ^{212}Bi [22], ^{212}At [23], ^{216}At [24], and ^{216}Fr [25] using alpha decay. Often it has been necessary to use alpha decaying parents which are in secular equilibrium with more massive alpha decaying parents because of extremely short half lives.

Figure 1 is a plot of energy versus spin of the $\pi 0h_{9/2}\otimes\nu 1g_{9/2}$ configuration for ^{210}Bi, ^{212}Bi, ^{212}At, ^{216}At, and ^{216}Fr. Experimental energies are connected by solid lines, and theoretical energies by dashed lines. These are theoretical results from this paper, which will be described later.

Figure 1 shows quite clearly that with the addition of pairs of neutrons or protons the inverted parabola structure of ^{210}Bi begins to flatten as the levels become more compressed. Ideally, one would want to go through a sequence of odd-odd nuclei such as ^{210}Bi, ^{212}At, ^{214}Fr, ^{216}Ac, and ^{218}Pa in which successive pairs of protons are added to ^{210}Bi. Similarly, the sequence ^{210}Bi, ^{212}Bi, ^{214}Bi, ^{216}Bi, and ^{218}Bi in which pairs of neutrons are added to ^{210}Bi would be of considerable interest. Perhaps the most interesting case would involve the study of the sequence ^{210}Bi, ^{214}At, ^{218}Fr, ^{222}Ac, and ^{226}Pa in which pairs of neutrons and protons are added. The hope in each of these cases is to study the configurations arising from pairs of protons added to the $0h_{9/2}$ orbital, pairs of neutrons added to the $1g_{9/2}$ orbital, and pairs of both protons and neutrons added to the $0h_{9/2}$ and $1g_{9/2}$ orbitals.

Unfortunately, we know that experimentally as we add the neutrons and protons, severe mixing begins to occur and ultimately we reach collective states arising from octupole-quadrupole deformed nuclei. This makes it impossible to follow the sequence of shell model configurations to their logical conclusion. Fortunately, however, theoretical calculations can avoid these difficulties by turning off mixing. It is the purpose of this paper to calculate the level structures of ^{212}Bi and ^{212}At with mixing, and then to turn off the mixing in order to calculate the sequence of shell model configurations in odd-odd nuclei in which the deformed collective effects are excluded. In order to achieve these ends, we present a description of the generalized intermediate coupling model (GICM).

II. THEORETICAL DESCRIPTION OF ODD-ODD SPHERICAL NUCLEI IN THE GICM

In the GICM [21], odd-odd nuclei are assumed to consist of a vibrating even-even core and two outer nucleons (odd proton and odd neutron). Thus, the model Hamiltonian can be written in the form

$$H_{\text{odd-odd}}=H_{\text{core}}+H_n+H_p+H_{n\text{core}}+H_{p\text{core}}+H_{np}, \quad (1)$$

where H_{core} is the Hamiltonian of the even-even core, H_n and H_p Hamiltonians of odd nucleons, $H_{p\text{core}}$ and $H_{n\text{core}}$ Hamiltonians of the interaction between the odd nucleons and the even-even core, and H_{np} Hamiltonian of the residual interaction between the odd neutron and the odd proton. Taking into account core vibrations does not improve the agreement to the experimental data for the studied nuclei. That is

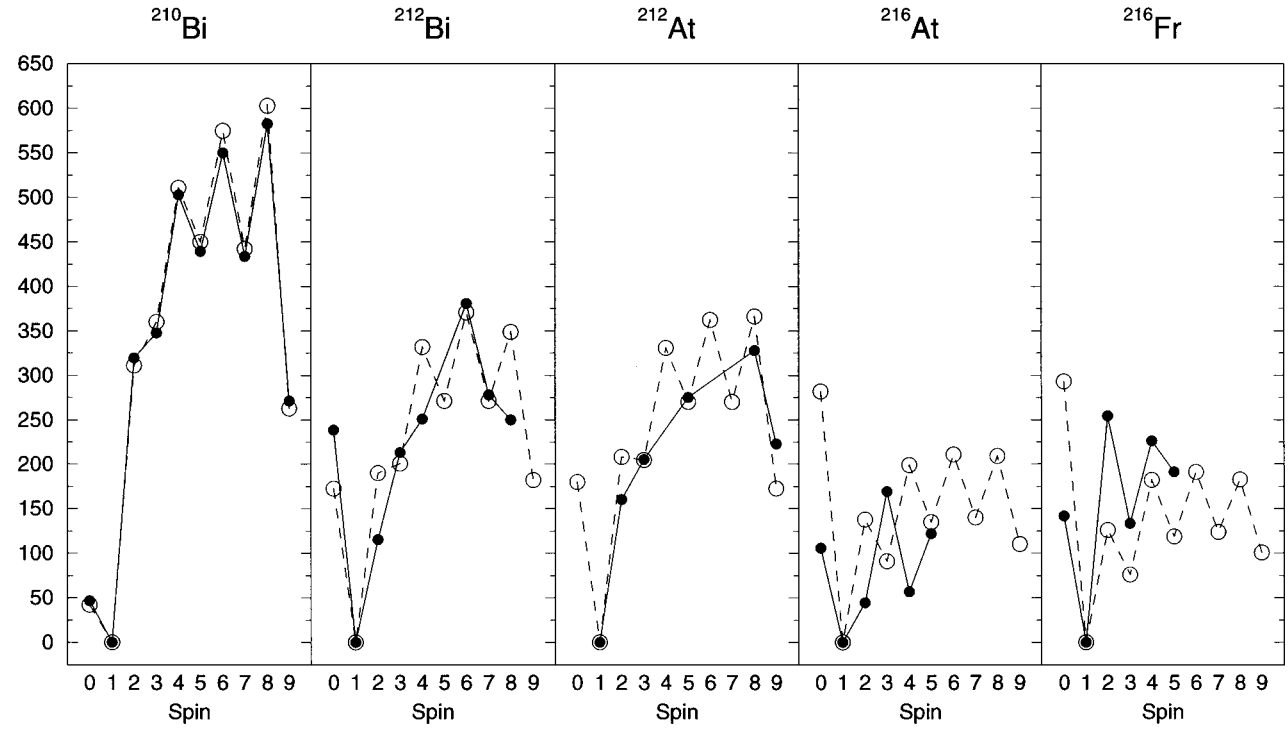

FIG. 1. Plot of the excitation energy vs spin of the $\pi 0h_{9/2}\otimes\nu 1g_{9/2}$ configuration for ^{210}Bi, ^{212}Bi, ^{212}At, ^{216}At, and ^{216}Fr. Experimental energies are shown as solid circles and connected by solid lines, and theoretical energies (from this paper) are shown as open circles and connected by dashed lines.

why we neglect in the model Hamiltonian $H_{\rm core}$, $H_{n\rm core}$, and $H_{p\rm core}$ in these calculations. For a description of one-quasiparticle neutron and proton states, the model of independent quasiparticles is used (H_n+H_p: spherical harmonic oscillator with spin-orbit interaction and l^2-term and monopole pairing interaction) [26]. In H_{np} (in the second quantization treatment) particle operators a, $a^\dagger$ are expressed in terms of quasiparticle operators α, $\alpha^\dagger$ with the help of the Bogoliubov transformation. The neutron-proton interaction (H_{np}) consists of the central part, noncentral tensor part, and spin-orbit part [27,28]:

$$H_{np}=V_c(r)(u_0+u_1\boldsymbol{\sigma}_p\cdot\boldsymbol{\sigma}_n+u_2P_M+u_3P_M\boldsymbol{\sigma}_p\cdot\boldsymbol{\sigma}_n)+V_t(r)\times(u_t+u_{tm}P_M)\left(\frac{1}{r^2}(\boldsymbol{\sigma}_p\cdot\boldsymbol{r})(\boldsymbol{\sigma}_n\cdot\boldsymbol{r})-\frac{1}{3}(\boldsymbol{\sigma}_p\cdot\boldsymbol{\sigma}_n)\right)+V_{ls}(r)(u_e^s+u_o^sP_M)\boldsymbol{l}\cdot\boldsymbol{s}, \quad (2)$$

where r is the distance between neutron and proton, $\boldsymbol{\sigma}_n$ and $\boldsymbol{\sigma}_p$ are Pauli spin matrices, P_M is the space exchange operator, $\boldsymbol{l}$ is the orbital angular momentum of the relative motion of proton and neutron, and $\boldsymbol{s}$ is the total spin of both nucleons. For $V_c(r)$, $V_t(r)$, and $V_{ls}(r)$ in Eq. (2) we use the Gaussian shape

$$V(r)=\exp(-r^2/r_0^2), \quad (3)$$

where $r_0=1.4$ fm. It means that a long-range n-p interaction is assumed.

The n-p interaction parameters are taken over from ^{210}Bi [21]. We have used 5 multiplets and 34 states in ^{210}Bi below 2 MeV. The multiplets and states are $\pi 0h_{9/2}\otimes\nu 1g_{9/2}$, $\pi 1f_{7/2}\otimes\nu 0i_{11/2}$ (9^- only), $\pi 0h_{9/2}\otimes\nu 0i_{11/2}$, $\pi 1f_{7/2}\otimes\nu 1g_{9/2}$, $\pi 0h_{9/2}\otimes\nu 0j_{15/2}$ (3^+–6^+, 12^+ only). We obtained the following set of parameters: $u_0=-40.4$ MeV, $u_1=-2.7$ MeV, $u_2=-32$ MeV, $u_3=-0.5$ MeV, $u_t=-73$ MeV, $u_{tm}=-108$ MeV, $u_e^s=-11$ MeV, $u_o^s=35$ MeV.

III. APPLICATION TO ^{212}Bi

The best models for calculation of ^{212}Bi are those taking into account four particle configurations (^{212}Bi has exactly four nucleons outside the doubly magic core) [29]. In our model, we are limited to two particle or two quasiparticle states. To approach the ^{212}Bi case, we have to use the following assumptions.

(1) An effective pairing interaction between valence neutrons is assumed. The effective neutron gap is estimated for the model core ^{210}Pb to be $\Delta_n=0.4$ MeV, since the first excited state at 0.8 MeV with spin 2^+ corresponds to a broken neutron pair out of the inert doubly magic ^{208}Pb.

(2) Neutron quasiparticle states in ^{211}Pb are calculated with the gap Δ_n. We start from the single-particle levels e_j from ^{209}Pb. To get rid of the chemical potential λ, the mean value of the valence neutrons is fixed

$$N=3=\sum_{j|m|}2v_j^2=\sum_{j|m|}\left(1-\frac{e_j-\lambda}{\varepsilon_j}\right), \quad (4)$$

ε_j is the quasiparticle energy

$$\varepsilon_j=[(e_j-\lambda)^2+\Delta_n^2]^{1/2}. \quad (5)$$

TABLE I. Parameters of the neutron (quasi-)particle states used for calculations of ^{212}Bi and ^{212}At. e_j stands for experimental single-particle neutron energies from ^{209}Pb, quasiparticle energies ε_j and amplitudes v_j have been calculated for ^{211}Pb, E_{expt} and E'_{expt} stand for the experimental energies of the states in ^{211}Pb and ^{211}Po, respectively. All energies are in keV. See text for more details.

Configuration	$e_j(^{209}\text{Pb})$	$\varepsilon_j(^{211}\text{Pb})$	$v_j(^{211}\text{Pb})$	$E_{\text{expt}}(^{211}\text{Pb})$	$E'_{\text{expt}}(^{211}\text{Po})$
$\nu 1g_{9/2}$	0	0	0.47	0	0
$\nu 0i_{11/2}$	779	638	0.18	639	687
$\nu 0j_{15/2}$	1423	1255	0.12	1303	1065
$\nu 2d_{5/2}$	1567	1395	0.11	1412	
$\nu 3s_{1/2}$	2032	1852	0.09	1722	
$\nu 1g_{7/2}$	2491	2305	0.07	2380	
$\nu 2d_{3/2}$	2538	2351	0.07	2512	

Then the quasiparticle energies ε_j and the amplitudes v_j for ^{211}Pb can be determined (see Table I). For comparison, experimental energies E_{expt} are also listed in Table I. It can be seen that a good agreement is obtained especially in the low excitation energy region.

(3) Proton states are taken from ^{209}Bi and are assumed to be only single particle (no proton pairing taken into account). Nevertheless, the spectra of ^{209}Bi and ^{211}Bi are quite different (see Table II). That is why in calculations for ^{212}Bi two sets of single-particle energies are used (one from ^{209}Bi and the other with the energy of the state $\pi 1f_{7/2}$ replaced by the experimental value from ^{211}Bi).

Results for ^{212}Bi are presented in Table III. E_A were calculated using the energy of the $\pi 1f_{7/2}$ state as 896 keV and E_B using this energy as 405 keV. The latter gives better results compared to the experimental data, but not as good as Warburton [29] for the ground-state multiplet $\pi 0h_{9/2} \otimes \nu 1g_{9/2}$. It can be seen from standard deviations 74 keV for E_A, 62 keV for E_B and 58 keV for Warburton. For E_A, $\pi 0h_{9/2} \otimes \nu 1g_{9/2}$ forms 95–100 % of the wave function; for E_B 88–100 % with the only exception of the 8^- state (48%) being strongly mixed with $\pi 1f_{7/2} \otimes \nu 1g_{9/2}$. When the energy of the $\pi 1f_{7/2}$ model state 405 keV is used, the multiplets $\pi 0h_{9/2} \otimes \nu 0i_{11/2}$ and $\pi 1f_{7/2} \otimes \nu 1g_{9/2}$ are strongly mixed.

The only fitted parameter (an overall energy shift to assure zero ground-state energy) was $E_0 = -0.44$ MeV, not far from the experimental value obtained from the binding energies (-0.51 ± 0.01) MeV.

IV. APPLICATION TO ^{212}At

^{212}At is a similar case to ^{212}Bi; only valence neutrons and protons are exchanged. We assume an effective pairing interaction between valence protons. The effective proton gap is estimated for the model core ^{210}Po to be $\Delta_p = 0.6$ MeV, since the first excited state at 1.2 MeV with the spin 2^+ corresponds to a broken proton pair out of the inert doubly magic ^{208}Pb. Proton quasiparticle states in ^{211}At are calculated with the gap Δ_p (analogous to ^{212}Bi), results are presented in Table II [now $Z = 3$ in Eq. (4) since ^{211}At has three valence protons]. From Table II, it can be seen that this assumption gives quite a good energy for the first excited state in ^{211}At. Neutron states are taken from ^{209}Pb and are assumed to be only single particle. Nevertheless, the spectra of ^{209}Pb and ^{211}Po are rather different (see Table I). That is why in calculations of ^{212}At two sets of single-particle energies are used (the first from ^{209}Pb and the second with the energies replaced by the experimental values from ^{211}Po).

Results are presented in Table III. E_C denotes model energies calculated using the single-particle neutron energies from ^{209}Pb and E_D with the single-particle neutron energies replaced by the experimental values from ^{211}Po. The latter give slightly better results compared to the experimental data. Nevertheless, the total agreement is not very good, since the calculated states especially of the second multiplet lie too high. The ground-state multiplet $\pi 0h_{9/2} \otimes \nu 1g_{9/2}$ is practically pure (maximum 10% admixtures of other multiplets) with no influence of the changed neutron single-particle energies. Multiplets $\pi 0h_{9/2} \otimes \nu 0i_{11/2}$ and $\pi 1f_{7/2} \otimes \nu 1g_{9/2}$ are mixed.

The only fitted parameter (an overall energy shift to assure zero ground-state energy) was $E_0 = -0.42$ MeV, not far from the experimental value (-0.49 ± 0.01) MeV.

V. APPLICATION TO ^{216}At AND ^{216}Fr

To calculate more complex nuclei like ^{216}At and ^{216}Fr with the simple model space of two quasiparticle states leads

TABLE II. Parameters of the proton (quasi-)particle states used for calculations of ^{212}Bi and ^{212}At. e_j stands for experimental single-particle proton energies from ^{209}Bi, quasiparticle energies ε_j and amplitudes v_j have been calculated for ^{211}At, E_{expt} and E'_{expt} stand for the experimental energies of the states in ^{211}Bi and ^{211}At, respectively. All energies are in keV. See text for more details.

Configuration	$e_j(^{209}\text{Bi})$	$E_{\text{expt}}(^{211}\text{Bi})$	$\varepsilon_j(^{211}\text{At})$	$v_j(^{211}\text{At})$	$E'_{\text{expt}}(^{211}\text{At})$
$\pi 0h_{9/2}$	0	0	0	0.48	0
$\pi 1f_{7/2}$	896	405	703	0.22	674
$\pi 0i_{13/2}$	1609		1371	0.14	
$\pi 1f_{5/2}$	2826		2556	0.09	

TABLE III. Comparison of the energies of the experimentally identified states in ^{212}Bi and ^{212}At multiplets to the model results with the Gaussian shape n-p interaction. E_{expt} and E'_{expt} stand for experimental energies from ^{212}Bi and ^{212}At, respectively. E_A denotes model energies calculated using the energy of the $\pi 1f_{7/2}$ state as 896 keV and E_B using this energy as 405 keV, E_W are taken from [29] (for ^{212}Bi). E_C denotes model energies calculated using the single-particle neutron energies from ^{209}Pb and E_D with the single-particle neutron energies replaced by the experimental values from ^{211}Po (for ^{212}At). Configurational assignment of the states in parentheses is uncertain. All energies are in keV.

Major configuration	I^π	$E_{\text{expt}}(^{212}\text{Bi})$	$E_A(^{212}\text{Bi})$	$E_B(^{212}\text{Bi})$	$E_W(^{212}\text{Bi})$	$E'_{\text{expt}}(^{212}\text{At})$	$E_C(^{212}\text{At})$	$E_D(^{212}\text{At})$
$\pi 0h_{9/2}\otimes\nu 1g_{9/2}$	0^-	238	180	173	220		180	180
	1^-	0	0	0	0	0	0	0
	2^-	115	211	190	186	160	208	208
	3^-	213	212	201	263	206	205	205
	4^-	251	336	332	319		331	331
	5^-		274	271	346	275	270	270
	6^-	381	373	371	345		362	362
	7^-	278	272	271	363		270	270
	8^-	250	386	349	303	328	366	366
	9^-		182	182	281	223	173	173
$\pi 0h_{9/2}\otimes\nu 0i_{11/2}$	1^-	415	405	297	(347)	(396)	1153	1071
	2^-	418	612	512	(654)	(623)	984	897
	3^-	(495)	848	925	(708)	(890)	1177	1101
	4^-		867	863	(870)	920	1094	1003
	5^-		945	966	(835)	1118	1172	1093
	6^-		872	871	(911)	(1210)	1075	985
	7^-		991	999	(731)	843	1177	1094
	8^-		748	775	(782)		995	906
	9^-		1030	1029	1080		1185	1094
	10^-		293	295	436	702	646	555
$\pi 1f_{7/2}\otimes\nu 1g_{9/2}$	1^-		1173	791	(511)	(55)	438	406
	2^-		1083	682	(703)	(364)	632	619
	3^-		1253	695	(826)	(783)	881	861
	4^-		1192	707	(936)	920	893	892
	5^-		1266	763	(899)	1118	978	966
	6^-		1157	668	(991)	(1089)	861	860
	7^-		1275	785	(863)	843	1017	1009
	8^-		916	432	(904)		506	505

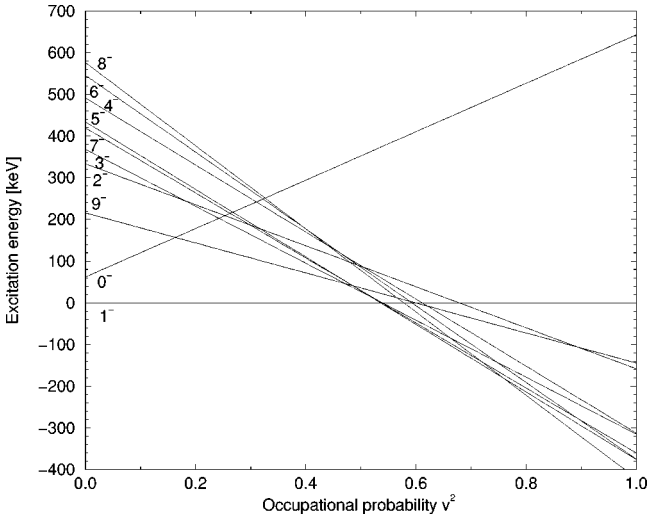

FIG. 2. Plot of the excitation energy vs the occupational probability v^2 for the $\pi 0h_{9/2}\otimes\nu 1g_{9/2}$ configuration. Only protons (or neutrons) fill the orbital; number of neutrons (protons) is fixed to be 1.

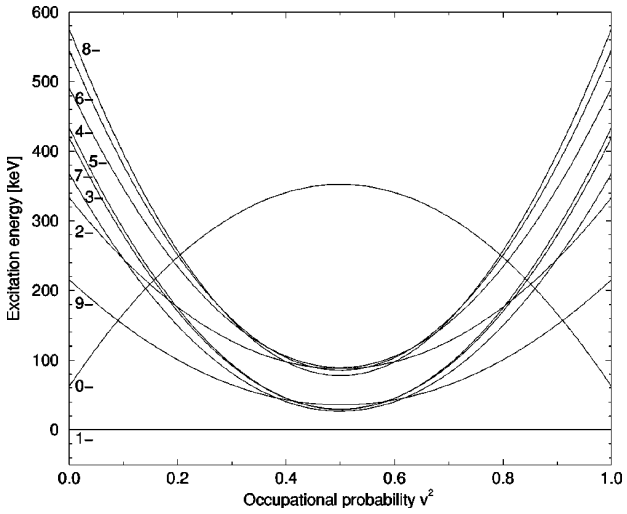

FIG. 3. Plot of the excitation energy vs the occupational probability v^2 for the $\pi 0h_{9/2}\otimes\nu 1g_{9/2}$ configuration. Both protons and neutrons fill the orbitals; the number of neutrons is the same as the number of protons that means the same occupational probability for protons and neutrons.

to less accurate results. Nevertheless basic trends can be reproduced. In Fig. 1 our results for the ground-state multiplet $\pi 0h_{9/2} \otimes \nu 1g_{9/2}$ with configurational mixing enabled are displayed and compared to the experimental energies. The gaps Δ_n and Δ_p were taken from Soloviev [26] ($\Delta_n = 0.7$ MeV, $\Delta_p = 0.6$ MeV for ^{216}At, and $\Delta_n = 0.55$ MeV, $\Delta_p = 0.8$ MeV for ^{216}Fr), neutron and proton single-particle energies were taken over from ^{209}Pb and ^{209}Bi, respectively, quasiparticle energies ε_j and occupational amplitudes v_j were calculated similarly as for ^{212}Bi and ^{212}At.

VI. CALCULATION OF CONFIGURATIONAL TRENDS

Using the GICM without mixing (only diagonal matrix elements of the model Hamiltonian taken into account), it is possible to simulate configurational trends beyond ^{208}Pb without the effects of deformation observed in the real experimental situation. In Figs. 2 and 3 we show the trends for the $\pi 0h_{9/2} \otimes \nu 1g_{9/2}$ configuration, adding either pairs of protons or pairs of neutrons in Fig. 2, and adding both pairs of neutrons and protons in Fig. 3. The reversal from the inverted parabola to the normal parabola is obvious in Fig. 2. In Fig. 3 one can see that we get the same inverted parabola again in the hole-hole limit.

VII. CONCLUSIONS

Recent experimental results on shell model configurations in odd-odd nuclei just beyond ^{208}Pb have been summarized. Experimentally, one observes inverted parabolas of energy versus spin plots which become more compressed as the number of nucleons is added beyond the closed shells in ^{208}Pb. However, it is impossible to follow the sequence of configurations to their ultimate limit in which particle-particle goes over into particle-hole, hole-particle, or hole-hole because deformation sets in, leading to an entirely different coupling scheme. Using the GICM, it is possible to reproduce the level structures of ^{210}Bi, ^{212}Bi, and ^{212}At reasonably well, and partially also ^{216}At, ^{216}Fr. Then by turning off the mixing one can show that the parabolic structures of energy versus spin reverse as one goes from particle-particle configurations to particle-hole or hole-particle configurations.

ACKNOWLEDGMENTS

Partial support from the State of Florida, the Grant Agency of the Czech Republic, and the Volkswagen Foundation is gratefully acknowledged.

[1] J. R. Erskine, W. W. Buechner, and H. A. Enge, Phys. Rev. **128**, 720 (1961).
[2] H. T. Motz, E. T. Jurney, E. R. Shera, and R. K. Sheline, Phys. Rev. Lett. **26**, 854 (1971).
[3] P. D. Ellegaard, P. D. Barnes, R. Eisenstein, and T. R. Canada, Phys. Lett. **35B**, 149 (1971).
[4] J. J. Kolata and W. W. Daehnick, Phys. Rev. C **5**, 568 (1972).
[5] C. K. Cline, W. P. Alford, H. E. Gove, and R. Tickle, Nucl. Phys. **A186**, 273 (1972).
[6] T. R. Canada, R. A. Eisenstein, C. Ellegaard, P. D. Barnes, and J. Miller, Nucl. Phys. **A205**, 145 (1973).
[7] D. Proetel, F. Riess, E. Grosse, R. Ley, M. R. Maier, and P. von Brentano, Phys. Rev. C **7**, 2137 (1973).
[8] D. J. Donahue, O. Hausser, R. L. Hershberger, R. Lutter, and F. Riess, Phys. Rev. C **12**, 1547 (1975).
[9] W. W. Daehnick, M. J. Spisak, R. M. Del Vecchio, and W. Oelert, Phys. Rev. C **15**, 594 (1977).
[10] W. W. Daehnick, M. J. Spisak, and J. R. Comfort, Phys. Rev. C **23**, 1906 (1981).
[11] R. L. Ponting, R. K. Sheline, E. T. Jurney, L. Nkwambiaya, and B. Bombaka, Rev. Zair. Sci. Nucl. **7**, 1 (1986).
[12] R. K. Sheline, R. L. Ponting, A. K. Jain, B. bu Nianga, and L. Nkwambiaya, Czech. J. Phys., Sect. B **39**, 22 (1989).
[13] N. Newby and E. J. Konopinski, Phys. Rev. **115**, 434 (1959).
[14] I. Yu. Kharitonov, L. A. Sliv, and G. A. Sogomonova, Nucl. Phys. **28**, 210 (1961).
[15] Y. E. Kim and J. O. Rasmussen, Nucl. Phys. **47**, 184 (1963).
[16] T. A. Hughes, R. Snow, and W. T. Pinkston, Nucl. Phys. **82**, 129 (1966).
[17] J. Vary and J. N. Ginocchio, Nucl. Phys. **A166**, 479 (1971); J. Vary, Ph.D. thesis, Yale University, 1970 (unpublished).
[18] G. H. Herling and T. T. S. Kuo, Nucl. Phys. **A181**, 113 (1972); T. T. S. Kuo and G. H. Herling, Memorandum No. 2258, Naval Research Lab, Washington, D.C., 1971 (unpublished).
[19] C. W. Ma and W. W. True, Phys. Rev. C **8**, 2313 (1973).
[20] E. K. Warburton and B. A. Brown, Phys. Rev. C **43**, 602 (1991).
[21] P. Alexa, J. Kvasil, M. Nguyen Viet, and R. K. Sheline, Phys. Rev. C **55**, 179 (1997).
[22] C. F. Liang, P. Paris, and R. K. Sheline, Phys. Rev. C **49**, 1872 (1994).
[23] C. F. Liang, P. Paris, R. K. Sheline, P. Alexa, and A. Gizon, Phys. Rev. C **54**, 2304 (1996).
[24] R. K. Sheline, C. F. Liang, and P. Paris, Phys. Rev. C **53**, 2152 (1996).
[25] R. K. Sheline, C. F. Liang, P. Paris, and A. Gizon, Phys. Rev. C **55**, 1162 (1997).
[26] V. G. Soloviev, *Theory of Complex Nuclei* (Pergamon Press, Oxford, 1976).
[27] J. P. Boisson, R. Piepenbring, and W. Ogle, Phys. Rep. **26**, 99 (1976).
[28] P. Ring and P. Schuck, *The Nuclear Many-Body Problem* (Springer, Berlin, 1980).
[29] E. K. Warburton, Phys. Rev. C **44**, 261 (1991).